# *Crosstalk of Ras and Rho: activation of RhoA abates Kras-induced liver tumorigenesis in transgenic zebrafish models*





| | |
|---|---|
| **Citation** | Chew, T. W., Liu, X. J., Liu, L., Spitsbergen, J. M., Gong, Z., & Low, B. C. (2014). Crosstalk of Ras and Rho: activation of RhoA abates Kras-induced liver tumorigenesis in transgenic zebrafish models. Oncogene, 33(21), 2717-2727. doi:10.1038/onc.2013.240 |
| **DOI** | 10.1038/onc.2013.240 |
| **Publisher** | Macmillan Publishers Limited |
| **Version** | Accepted Manuscript |
| **Terms of Use** | http://cdss.library.oregonstate.edu/sa-termsofuse |

# Crosstalk of Ras and Rho: activation of RhoA abates Kras-induced liver tumorigenesis in transgenic zebrafish models

**Ti Weng Chew[1,2], Xing Jun Liu[3], Lihui Liu[1], Jan M. Spitsbergen[4], Zhiyuan Gong[3], Boon Chuan Low[1,2*]**

[1] Cell Signaling and Developmental Biology Laboratory, Department of Biological Sciences, The National University of Singapore, Singapore 117543, The Republic of Singapore

[2] The Mechanobiology Institute, Singapore, National University of Singapore, T-Lab, 5A Engineering Drive 1, Singapore 117411, The Republic of Singapore

[3] Molecular Biology Laboratory, Department of Biological Sciences, The National University of Singapore, Singapore 117543, The Republic of Singapore

[4] Department of Microbiology and Marine and Freshwater Biomedical Sciences Center, Oregon State University, Corvallis, Oregon, USA

* Corresponding author:

Dr. Boon Chuan LOW (dbslowbc@nus.edu.sg)

Tel: 65-6516-7834

Fax: 65-6779-2486; 65-6872-6123

**Abstract**

RAS and Rho small GTPases are key molecular switches that control cell dynamics, cell growth and tissue development through their distinct signaling pathways. While much has been learnt about their individual functions in both cell and animal models, the physiological and pathophysiological consequences of their signaling crosstalk in multi-cellular context *in vivo* remain largely unknown, especially in liver development and liver tumorigenesis. Furthermore, the roles of RhoA in RAS-mediated transformation and their crosstalk *in vitro* remain highly controversial. When challenged with carcinogens, zebrafish developed liver cancer that resembles the human liver cancer both molecularly and histopathologically. Capitalizing on the growing importance and relevance of zebrafish (*Danio rerio)* as an alternate cancer model, we have generated liver-specific, Tet-on inducible transgenic lines expressing oncogenic $Kras^{G12V}$, RhoA, constitutively-active $RhoA^{G14V}$ or dominant-negative $RhoA^{T19N}$. Double transgenic lines expressing $Kras^{G12V}$ with one of the three RhoA genes were also generated. Based on quantitative bioimaging and molecular markers for genetic and signaling aberrations, we showed that the induced expression of oncogenic Kras during early development led to liver enlargement and hepatocyte proliferation, associated with elevated Erk phosphorylation, Akt2-p21Cip expression and activation. Such an increase in liver size and Akt2 expression was augmented by dominant-negative $RhoA^{T19N}$, but was abrogated by the constitutive-active $RhoA^{G14V}$. Consequently, induced expression of the oncogenic Kras in adult transgenic fish led to the development of hepatocellular carcinomas. Survival studies further revealed that the co-expression of dominant-negative $RhoA^{T19N}$ with oncogenic Kras increased the mortality rate compared to the other single or double transgenic lines. This study represents the first *in vivo* investigation of the previously unappreciated signaling crosstalk between Kras and RhoA in regulating liver overgrowth and liver tumorigenesis. Our results also implicate that activating Rho could be beneficial to suppress the Kras-induced liver malignancies. (290 words)

**Keywords:** hepatocellular carcinoma, zebrafish, RhoA, Ras, signaling crosstalk, Akt

## Introduction

Aberrant RAS signaling were found in up to 30% of all human cancers (1). In particular, activating mutation such as G12V diminishes the ability of the RAS small GTPase to hydrolyse the bound GTP to GDP, thus rendering it constitutively active. Of the three RAS isoforms, KRAS is most frequently mutated in human cancers (2). For example, organs forming the digestive system are strongly associated with Kras mutation, with the pancreas being highly targeted (3). Some human liver cancers were also found to harbour activating mutation of the KRAS gene (4). Hepatocellular carcinoma (HCC), which accounted for 70 to 85% of deaths linked to liver cancer (5), was ranked third in the causes of cancer mortality (6). HCC is highly associated with hepatitis B or C viral infection, aflatoxin ingestion, alcoholism, and cirrhosis-inducing conditions (7). At the molecular level, several altered/aberrant signaling pathways that engage RAS or its effectors have been implicated in the development and progression of HCC (8, 9), suggesting the importance of RAS in liver transformation. The Raf/MAPK and PI3K/Akt cascades are two such downstream effectors of RAS signaling that were largely implicated in many RAS-driven tumorigenesis (1, 4). Until recently, only one such animal model of RAS-driven HCC has been reported: transgenic mice expressing $HRAS^{G12V}$, together with the loss of β-catenin signaling, in the liver developed HCC (10). However, there is still a serious lack of appropriate animal models for studying RAS-driven HCC that would permit more systematic analyses on their impact under different genetic perturbations and signalling crosstalk, especially by Rho.

RhoA, a member of the RHO small GTPase family, is highly homologous to the RAS. They are also key molecular switches that regulate cell dynamics, cell growth and tissue development. However, unlike activating mutations of RAS, the expression levels and overall activity of RhoA were found to be elevated in many human tumors, including liver cancer (11). Indeed, RhoA has been suggested to be a suitable prognostic marker for HCC (12-14). These observations suggested the importance of RhoA in the formation and progression of liver malignancies.

While much has been learnt about their individual functions and crosstalk *in vitro*, the physiological/pathophysiological consequences of their signaling crosstalk *in vivo* remains largely unknown. In addition, the roles of RhoA in RAS-mediated transformation and their

crosstalk *in vitro* remain controversial. Many pioneering *in vitro* studies reported an elevated level of RhoA and/or RhoA activities in oncogenic RAS-transformed cells or a requirement of RhoA signaling for RAS-mediated transformation (15-21). Conversely, there were also studies that reported the down-regulation or non-involvement of RhoA or RhoA effectors in oncogenic RAS-transformed cells (22-25) (see Table S1 for a summary of these studies). As such, the underlying molecular mechanism of signaling crosstalk between RhoA and RAS is still not well-defined. Adding to the complexity, it appears that certain crosstalks are cell-type-specific, vary with the RAS subtype, and depend on the kinetics and duration of RAS activation (16).

Zebrafish, *Danio rerio*, is fast becoming a popular animal model for studying human cancers (26-29). This is primarily attributed to its low cost of zebrafish husbandry, rapid development, high fecundity, amenability to reverse and forward genetics, low incidence of spontaneous tumors, ease of application of small chemical molecules and small size of all life stages. Most importantly, carcinogen-treated zebrafish developed liver tumors that resemble human liver cancers both molecularly and histologically (29, 30). Our laboratories have recently established the zebrafish as a model for studying small GTPase signaling (31-34) and have also generated Kras transgenic lines under the constitutive expression and mifepristone-inducible system to induce HCC, respectively (35, 36). These make zebrafish a suitable model for a more systematic study of liver development and HCC driven by the oncogenic small GTPases.

Here, we report the generation of the first tetracycline-inducible (Tet-on) zebrafish HCC model driven by oncogenic Kras signaling. This system eliminates the need for the crossing of the driver and effector lines, and the zebrafish has higher tolerance for doxycycline than mifepristone as the inducer. Furthermore, transcriptomic analysis carried out on the mouse liver suggested that the Tet-on system was safer than the mifepristone-inducible system because of its smaller effect on the transcriptome (37). We showed that induced expression of the $Kras^{G12V}$ caused liver enlargement, concomitant with increased Raf/MAPK and PI3K/Akt activation. The $Kras^{G12V}$ expression in adult transgenic also led to the development of HCC associated with increased Raf/MAPK signaling. In the double-transgenic lines, the $Kras^{G12V}$-mediated liver overgrowth was augmented significantly by the dominant-negative mutant of $RhoA^{T19N}$, but was significantly reduced by the constitutively active $RhoA^{G14V}$. This result could in part, be attributed to the regulation of Akt2 expression and activation in the respective double transgenic

lines. Survival studies further revealed that co-expression of RhoA$^{T19N}$ with oncogenic Kras increased the mortality rate significantly as compared to other single or double transgenic lines.

## Results

### Characterization of an inducible, liver-specific transgenic Kras$^{G12V}$ line of zebrafish

To validate the Tet-on inducible and liver-specific expression of the Kras$^{G12V}$, doxycycline induction was performed. Liver-specific EGFP signal was observed in the transgenic larva (Figure 1A), arising from the induced EGFP-Kras$^{G12V}$ expression (Figure 1B) while Ras activation assay confirmed that the ectopically expressed EGFP-Kras$^{G12V}$ retained its active-form (Figure 1C). KRAS, like HRAS and NRAS, had to be plasma membrane-bound for effective signaling to take place especially during growth and transformation-related processes (38). Figure 1D illustrated that EGFP-Kras$^{G12V}$ were enriched at the hepatocytes' plasma membrane. All these results therefore confirm that the Kras transgene expression is liver-specific and faithfully recapitulates its activity *in vivo*. The *TO(Kras$^{G12V}$)* was further examined for their impacts on liver development and cancer.

### Kras G12V induces liver overgrowth by increasing hepatocyte proliferation

To study the impacts of Kras$^{G12V}$ on liver growth, volumetric analysis of the liver in *TO(Kras$^{G12V}$)* larvae were performed. It was shown that the liver of the *TO(Kras$^{G12V}$)* larvae were significantly larger than that of the control by 2-fold (Figure 2A). The Lipan line (39), which expresses dsRED in the liver specifically, was used as the control because of the need for fluorescence labeling. To minimize the genetic and environmental background variations, *TO(Kras$^{G12V}$)* was crossed to the Lipan. The double-transgenic and Lipan were used to represent the *TO(Kras$^{G12V}$)* and wild-type population, respectively. To determine whether the liver overgrowth was due to any increase in proliferation, immunostaining for phospho-histone 3 (pH3), a mitosis marker, was performed. The hepatocyte proliferation rate was significantly higher in the *TO(Kras$^{G12V}$)* than those in the controls (Figure 2B), indicating that the expression of Kras$^{G12V}$ resulted in increased hepatocyte proliferation.

**Ectopically expressed Kras$^{G12V}$ activates RAF/MEK/ERK and PI3K/AKT pathways**

Next, we examined whether the liver overgrowth and increased proliferation were associated with the activation of RAF/MEK/ERK and/or PI3K/AKT. Figures 3A and 3B demonstrated that the activities of the RAF/MEK/ERK and PI3K/AKT pathways were indeed increased in the *TO(Kras$^{G12V}$)* compared to their wild-type siblings, as shown by the increased levels of phospho-Erk and phospho-Akt2, respectively. The protein level of Akt2 was also increased in *TO(Kras$^{G12V}$)* compared to the wild-type control. Moreover, an elevated level of phospho-p21Cip (a substrate of activate Akt) was observed in the transgenic larvae compared to the wild-type (Figure 3C). Altogether, the ectopically-expressed Kras$^{G12V}$ led to an increase in RAF/MEK/ERK and PI3K/AKT/p21Cip signaling which could lead to increased hepatocyte proliferation and liver enlargement.

**Kras$^{G12V}$ induces HCC *in vivo***

Since induced Kras$^{G12V}$ expression caused liver enlargement in the transgenic larvae, we examined whether it could result in liver malignancies in the adult *TO(Kras$^{G12V}$)*. Indeed, the induced expression of Kras$^{G12V}$ resulted in liver overgrowth (Figure 4A) compared to the control (Figures 4B & 4C). Diagnosis by H&E-stained sections revealed the development of liver malignancies that displayed features characteristic of HCC in the *TO(Kras$^{G12V}$)* (Figure 4D) but not in the controls (Figure 4E & F). Immunohistochemical staining for PCNA, a proliferation marker, further illustrated the higher proliferation rate in Kras$^{G12V}$-mediated HCC (Figure 4G) than in the controls (Figure 4H and I). To examine the significance of the RAF/MEK/ERK in the HCC development, immunostaining probing for phospho-ERK1/2 was performed. Enhanced nuclear staining of phospho-Erk1/2 was observed in the HCC sample (Figure 4J) compared to the control (Figure 4K), indicating an increase in MEK/Erk activation. Interestingly, the upregulation of the MEK/Erk signaling was more intense at the periphery than that in the centre of the liver (HCC sample), revealing possible physical and mechanical influence on the spatial activation of Ras/MAPK *in vivo* (Figure S1).

**Functional crosstalk of Ras and Rho *in vivo*: the differential impacts of RhoA signaling on $Kras^{G12V}$-mediated liver overgrowth and its association with Akt2 signaling**

Next, we determined the possible functional crosstalk of Kras and RhoA, and their physiological impacts on liver overgrowth and liver tumorigenesis. Three Tet-on inducible, liver-specific transgenic lines expressing wild-type RhoA, constitutive-active $RhoA^{G14V}$ and dominant-negative $RhoA^{T19N}$, were generated. The transgenic larvae expressed the mCherry-tagged proteins in the liver upon doxycycline induction (Figure 5A to C), respectively. Western analyses revealed that the RhoA transgenes were expressed faithfully as mCherry-tagged proteins. Micrographs of cryostat sections (Figures 5G to I) further illustrated the liver-specific expression of the mCherry-tagged proteins. Inducible double-transgenic lines expressing both the Kras and the RhoA were derived through the careful crossing/breeding of the selected transgenic lines (Figure S2).

As described earlier, the liver-specific expression of $Kras^{G12V}$ caused liver overgrowth in the *TO($Kras^{G12V}$)* larvae, accompanied by elevated expression of Akt2 and inactivation of its downstream target, p21Cip (Figure 3). Since PI3K/Akt signaling is important for liver growth and regeneration (40, 41), and potentially a key therapeutic target and biomarker of liver malignancy (42-44), we investigated the impacts of this functional crosstalk between Kras and RhoA on the regulation of Akt signaling. Figure 6A shows that co-expression of $RhoA^{T19N}$ with $Kras^{G12V}$ augmented $Kras^{G12V}$-mediated liver overgrowth significantly. And this apparent synergism in the *TO($Kras^{G12V}$/$RhoA^{T19N}$)*, when compared to the *TO($Kras^{G12V}$)*, was accompanied by a further increase in the expression (panel 3, Figure 6D) and the overall activation level of Akt2 (top panel, Figure 6D; lower exposure shown as second panel). However, expression of $RhoA^{T19N}$ alone did not affect the liver size (Figure S3B), the steady state levels of Akt2 expression and its activity (Figure 6D).

In contrast, when compared to the *TO($Kras^{G12V}$)*, co-expression of $RhoA^{G14V}$ reduced the $Kras^{G12V}$-mediated liver enlargement significantly (Figure 6B) whereas no significant changes in the liver size (Figure 6C) or the expression level/activity of Akt2 (Figure 6F) were observed when the wild-type RhoA was co-expressed in the *TO($Kras^{G12V}$/RhoA)* larvae. Strikingly, such an antagonistic effect of $RhoA^{G14V}$ on $Kras^{G12V}$ was associated with an inhibition of both the expression level (panel 2, Figure 6E) and the activities of Akt2 (top panel, Figure 6E).

Furthermore, all the changes in liver size in these double-transgenic lines were correlated to the changes in hepatocyte proliferation (Figure S3A). Similar to *TO(RhoA$^{T19N}$)*, expression of RhoA$^{G14V}$ alone did not cause any significant change to the liver size as compared to the control (Figure S3B). Taken together, all these results provide the first *in vivo* evidence that changes in Rho signaling could antagonize or potentiate the impacts of active Ras-Akt2 signaling in controlling liver growth, thus offering suitable models to further elucidate their impacts on liver tumorigenesis.

**Impacts of RhoA signaling on Kras$^{G12V}$-mediated liver tumorigenesis**

Next, we investigated the effects of RhoA signaling on Kras$^{G12V}$-mediated liver tumorigenesis. From the survival curves in Figure 7A, we observed the following: (1) 100% of the wild-type control and single RhoA transgenic fish survived the induction treatment, (2) induction of Kras$^{G12V}$ expression in the liver caused a significant decrease in survival compared to the wild-type, (3) co-expression of RhoA or RhoA$^{G14V}$ with Kras$^{G12V}$ did not cause any significant changes to the survival rate compared to *TO(Kras$^{G12V}$)*, (4) co-expression of RhoA$^{T19N}$ with Kras$^{G12V}$ led to a significant increase in death rate compared to the *TO(Kras$^{G12V}$)*, *TO(Kras$^{G12V}$/RhoA)* and *TO(Kras$^{G12V}$/RhoA$^{G14V}$)*. The increased mortality of *TO(Kras$^{G12V}$/RhoA$^{T19N}$)* correlated well with the increased liver overgrowth and proliferation compared to the *TO(Kras$^{G12V}$)* (Figure 6A and S3A) in the larval stage. No deaths were observed in the non-induced control groups.

To verify the major causes of death from the treatment, post-mortem sampling of "dead" fish for histopathological diagnoses were performed and all were diagnosed with liver lesions that were characteristic of liver tumors, with the most serious form being HCC (Figure 7B-I). There were no significant differences in the severity of the liver lesions between the three double transgenic lines compared to the *TO(Kras$^{G12V}$)*, as determined by *Fisher's exact test* (Table S2). Also no fish in any treatment group had HCC at more advance stage than grade 2. All of the *TO(Kras$^{G12V}$/RhoA$^{T19N}$)* transgenic fish were diagnosed with HCC. Apparently, they also demonstrated higher proliferation activity (Figure 7K) than those in the other three genotypes analysed (Figure 7J, L and M). The induction of RhoA, RhoA$^{G14V}$ or RhoA$^{T19N}$ expression alone

did not result in any death (Figure 7A), liver enlargement or formation of malignant liver lesion (Figure S4).

## Discussion

### $Kras^{G12V}$ induces liver overgrowth by activation of Ras/Erk and PI3K/Akt2/p21Cip

RAS GTPases are key regulators of cell growth, survival and differentiation. Our present study shows that the liver-specific expression of the $Kras^{G12V}$ increases hepatocyte proliferation leading to liver overgrowth, in a process accompanied by increased Raf/MAPK and PI3K/Akt2 signaling. Increased Raf/MAPK and PI3K/AKT signaling are frequently found in many human cancers (2, 45). In addition, we also observed an increase in Akt2 expression in the *TO(*$Kras^{G12V}$*)* compared to the control. Akt2 expression level is consistently up-regulated in many human cancers and correlated to higher pathological grade tumors, for example, HCC, colon cancers, squamous cell carcinomas, and gliomas (46-49). Furthermore, p21Cip is found to be inactivated by heightened Akt2-mediated inhibitory phosphorylation of the p21Cip protein. Phosphorylation of p21Cip at threonine 145 is a negative regulator of its function and disrupt the inhibitory interaction with proliferating cell nuclear antigen (PCNA) (50-52), thus promoting proliferation and cell survival. Such phosphorylation by AKT also causes the protein to reside in the cytosol, thus preventing its inhibitory interaction with the cyclin-dependent kinase (CDK) or PCNA (53). Taken together, the *TO(*$Kras^{G12V}$*)* offers a suitable model for studying oncogenic Kras signaling as it faithfully recapitulates major signaling pathways perturbed by activating mutation of RAS. Indeed, we have provided the first evidence here that the active RhoA could suppress the induction of Akt expression by $Kras^{G12V}$, and thus suppresses liver enlargement and proliferation of hepatocytes whereas its dominant-negative form augments the effects of Kras in all those processes, leading to greater mortality rates (see later part of discussion).

### $Kras^{G12V}$ promotes development of HCC in adult zebrafish.

Activating mutation of Kras plays a central role in the progression of many human cancers. Here, we show that induced expression of $Kras^{G12V}$ in the liver led to the formation of

HCC, with increased proliferation and Ras/Erk activities. The phospho-Erk1/2 were largely localized to the nucleus, consistent with the view that the activated Erk1/2 needs to translocate to the nucleus for activating the transcription factors for mitogenic responses (54). Impaired nucleus translocation of activated Erk1/2 (cytosolic retention) not only reduced cell proliferation and survival signals, but can also activate death-associated protein kinase to promote apoptosis (54). Interestingly, we have reported a spatial regulation of Erk1/2 activation which could be attributed to the interplay of physical and biological signals. Similar spatial regulation of ERK phosphorylation/activation is reported recently in an *in vitro* study using epithelial cells as the model (55). These findings further illustrate the relevance of the *TO(Kras$^{G12V}$)* as a model for Kras$^{G12V}$-driven HCC.

**Distinct impacts of RhoA on Kras$^{G12V}$-mediated liver overgrowth and tumorigenesis.**

Crosstalk of RAS and RhoA in regulating tumorigenesis, largely studied in *in vitro* systems, remains controversial with the majority suggesting that RhoA signaling enhanced RAS-driven transformation or RAS-driven transformation necessitate RhoA signaling input. Our findings provide the first evidence for the functional crosstalk of RAS and Rho in an *in vivo* animal model. We showed that the expression of the dominant-negative RhoA$^{T19N}$ augments Kras$^{G12V}$-mediated liver overgrowth, HCC development and cancer mortality. And in strong contrast, the expression of constitutively-active RhoA$^{G14V}$ helped suppress Kras$^{G12V}$-driven liver overgrowth in the larvae at least through a reduction in Akt2 expression and activation with a concomitant reduction in hepatocyte proliferation. These results suggest that active RhoA plays an important inhibitory role in Kras oncogenic signaling. Consistent with our *in vivo* data, constitutive-active RhoA has been shown to inhibit AKT activation through the Rho kinase-dependent pathway (56). Moreover, activation of RhoA by vasopressin (vasoactive peptide hormone) can downregulate cyclin-D1 expression, leading to the inhibition of oncogenic Kras-driven proliferation (57). In another study, it was demonstrated that RhoA$^{G14V}$ could inhibit proliferation by slowing down G1 to S phase cell cycle transition and hindering the completion of cytokinesis (58).

It is worth noting that many studies which demonstrate the requirement of active RhoA in RAS transformation, utilize the HRAS isoform instead of the KRAS isoform (Table S1). Furthermore, all except the study by Vidal and colleagues (2002), use a fibroblast cell-type instead of epithelial cell-type to which the hepatocytes belong (15-19, 21, 59-62). The fibroblast cell-type responds differently from the epithelial cell-type when activated RAS is introduced. Thus the fibroblast may be an inappropriate model for RAS-induced transformation (63). Other reports support our finding that RhoA signaling does not augment or support Ras transformation (23, 25, 64, 65) . Interestingly, two out of these studies that supported our findings employed the KRAS mutants in their experimental setup, and one of these two studies utilized an epithelial cell-type for their investigation (23, 65). It was suggested that this crosstalk of RAS and Rho depend on cell-types, RAS isoforms, and duration of RAS activation (16). All the studies above were conducted in an *in vitro* cell-based setting. Therefore, it is of paramount importance that we addressed this crosstalk of Kras and RhoA in an *in vivo* animal model.

In summary, this study represents the first *in vivo* investigation of the previously unappreciated signaling crosstalk between Kras and RhoA in regulating liver overgrowth, hepatocytes transformation and cancer mortality. Specifically, such an inducible transgenic system offers an exciting platform for modeling human HCC, and as an alternative *in vivo* model for studying the physiological roles of small GTPase signaling and their possible inter-play in regulating normal organ development and disease manifestation. In this context, we showed that halting RhoA signaling could augment Kras-mediated liver overgrowth and tumorigenesis. These data could have far reaching influence on the development and application of therapeutics directed at inhibiting RhoA signaling in KRAS-driven tumors. Furthermore, our results implicate that activating Rho could be beneficial to suppress Kras-induced liver malignancies.

## Materials and Methods

### Zebrafish maintenance

Zebrafish were maintained in compliance with the Institutional Animal Care and Use Committee (IACUC) guidelines of National University of Singapore.

### Generation of the *Tg(fabp10:rtTA2s-M2;TRE2:EGFP-kras$^{G12V}$)* zebrafish

Transgenic founders were created by the co-injection of linearized p*fabp10*-rtTA2s-M2 [*fabp10* promoter (66) upstream of rtTA2s-Ms] (67) and pTRE2-eGFP-Kras$^{G12V}$ into one cell embryo. Zebrafish *kras* gene was described in (33) and site-directed mutagenesis performed on pGEM-T *kras* with primer pair GTGGTCGTGGGAGCTGTCGGCGTAGGCAAAAGC and GCTTTTGCCTACGCCGACAGCTCCCACGACCAC to obtain pGEM-T *Kras$^{G12V}$* (Site-directed mutagenesis kit, Agilent, La Jolla, CA, USA). The *kras$^{G12V}$* was subcloned into pTRE2-EGFP vector. Injected embryos were raised to adulthood. Potential F0 fish were screened by out-crossing to wild-type stock. One F0 fish was identified and used to establish the stable transgenic line *Tg*(*fabp10:rtTA2s-M2;TRE2:EGFP-kras$^{G12V}$*), named *TO(kras$^{G12V}$)* in this communication (Figure S5A).

### Generation of the *Tg(fabp10:rtTA2s-M2:TRE2:mCherry-rhoA)* zebrafish

*mCherry* and *rhoA* genes were subcloned into pTRE2 vector (Clontech, Mountain View, CA, USA) from the pmCherry vector (Clontech, Mountain View, CA, USA) and pCS2+ *rhoA** vector (32), respectively. The *rhoA** represents the wild-type *rhoA*, constitutive-active *rhoA$^{G14V}$* or the dominant-negative *rhoA$^{T19N}$* in this communication for ease of presentation. Subsequently, the *fabp10*-rtTA2s-M2 and TRE2-mCherry-*rhoA** were subcloned into the pDS vector (68) to yield pDS-*fabp10*-rtTA2s-M2-TRE2-mCherry-*rhoA** vector. Transgenic *rhoA* zebrafish were generated using the *Ac/Ds* transposon system as described previously (68) by co-injection of plasmid with *Ac* mRNA into one-cell stage embryo. Microinjected embryos were raised to adulthood and screened for founders. One founder was selected from each *rhoA* group to establish the stable line for each line (Figure S5B). The RhoA stable transgenic lines were named

*TO(RhoA*)* in this communication. Progeny derived from the crossing between the *TO(kras$^{G12V}$)* and *TO(RhoA*)* were subsequently named *TO(Kras$^{G12V}$/RhoA*)*.

**Induction of transgene expression with doxycycline**

Two dpf larvae were treated with doxycycline (20 μg/ml) (Sigma-Aldrich, St Louis, MO, USA) and screened for fluorescence (EGFP or mCherry) at five dpf by fluorescence microscopy. Larvae were sorted according to the expression of difference fluorescence (EGFP and/or mCherry). They were documented with Zeiss Axio Vert microscope (Carl Zeiss, Germany).

For the induction study, approximately three months old fish were used. Eight different genotypes, each divided in two groups (treated vs control; 40 fish each) were studied. They were housed in tank with five fish to one liter of water aerated with an air-pump. Tanks were housed in the dark throughout the treatment. Water was changed every other day, and dosed with doxycycline (10 μg/ml) for the treatment group and none for the control. Death events were defined as follows: (1) dead and rotten (2) freshly dead and (3) near-dead fish. The near-dead fish were sacrificed. Survival analysis by log rank test was performed with GraphPad Prism 5 (GraphPad Software, La Jolla, CA, USA). Differences were considered significant at p-value < 0.01. Dead/sacrificed fish were sampled for histopathological diagnoses. The tumor incidences were analysed statistically at p-value < 0.05 by Fisher's exact test.

**Confocal microscopy-volumetric analysis of the larvae liver**

Six dpf larvae were fixed overnight in 4 % paraformaldehyde (Sigma-Aldrich, St Louis, MO, USA) at 4 $^{o}$C. Fixed larvae were washed with PBST and cleared in a progressive increment of glycerol from 10% to 50% in PBS. They were stored overnight in 50 % glycerol/PBS/2.5 % 1,4-Diazabicyclo[2.2.2]octane (DABCO) (Sigma-Aldrich, St Louis, MO, USA) at 4 $^{o}$C. Larvae were mounted onto glass-based dish (Iwaki, Japan) in aqueous mounting media (50 % glycerol, PBS, 7.5 % gelatin, 2.5 % DABCO) for documentation. Images (Z-stack; lateral) were documented by Lecia MP 5x microscopy (Lecia, Germany). Image processing was subsequently performed with IMARIS, (Bitplane AG, Switzerland). Briefly, images were converted to Imaris

format and viewed in Surpass model. Surfaces were created and volumes occupied by the fluorescence signals were estimated by the surface creation wizard. *T*-tests were performed to determine differences statistically at p-value < 0.01.

**Immunostaining of cryostat section**

Cross sections of 10 μm were cut using a cryostat-microtome (Lecia, USA) following the protocol described in (31, 69). Slides were washed in PBS, and were either stained with DAPI (Life technologies, Carlsbad, CA, USA) and mounted for direct viewing or used for immunostaining. For immunofluorescence, the sections were blocked and permeabilised with blocking solution (5 % goat serum/PBS/0.3 %Triton-X100). Anti phospho-histone3 antibody (1:200) (Millipore, Billerica, MA, USA) in blocking solution was applied and incubated at 4 $^{o}$C overnight. The slides were washed thrice in PBS. Alexa fluor 647 antibody (1:200) (Life technologies, Carlsbad, CA, USA) were applied and incubated for two hours at room temperature. Slides were washed thrice in PBS, counter-stained with DAPI and mounted with fluorsave (Calbiochem, San Diego, CA, USA). Images were captured with Zeiss LSM510 Meta microscopy (Carl Zeiss, Germany) or Lecia MP 5x and analysed with ImageJ (National Institutes of Health, Bethesda, Maryland, USA). Differences were considered significant at p-value < 0.05 by *T*-test.

**Histological preparation and analyses**

Live adult fish were anaesthetized in 0.5 % phenoxyethanol (Sigma-Aldrich, St Louis, MO, USA ), sacrificed and fixed in Bouin's fixative (saturated picric acid: 37 % formalin : acetic acid, 15:5:1) (Sigma-Aldrich, St Louis, MO, USA) for four days at room temperature. Dead fish were fixed directly. The fixed specimens were embedded in paraffin (Sigma-Aldrich, St Louis, MO, USA). Sectioning of paraffin blocks into five μm section (sagittal) and H&E staining were prepared by Biopolis-Shared-Facilities (IMCB, Singapore). Histopathological diagnoses on the H&E slides were performed to determine the presence of liver lesion based on criteria described previously (30, 70, 71).

**Immunostaining of paraffin section**

Sections were deparaffined and rehydrated, and heat-processed in antigen retrieval solution (10 mM sodium citrate buffer pH 6.0, 0.5 % Tween 20). Processed slides were used either for immunohistochemical (IHC) or immunofluorescence staining.

IHC was performed with EnVision+ HRP system (DAKO, Denmark). Sections were treated with Dako peroxidase block for 15 minutes, and followed by one hour of incubation with blocking buffer (10 % goat serum/TBS/1 % BSA). Anti-PCNA (1:75) (Santa Cruz Biotechnology, Santa Cruz, CA, USA) in 1 % BSA/TBS were applied and incubated at 4 $^{o}$C overnight. Slides were washed in TBST and incubated at room temperature with Dako polymer/HRP for 30 minutes. Slides were washed in TBST, developed with Dako DAB+ staining buffer, counterstained with hematoxylin, and mounted with Permount (Fisher Scientific, Rockford, IL, USA). Documentation was performed using the Zeiss Axioskop2 microscopy (Carl Zeiss, Germany). For immunofluorescence study, the peroxidase blocking step was omitted and the polymer/HRP was replaced with Alexa fluor 488 and/or Alexa fluor 546 (1:200) (Life technologies, Carlsbad, CA, USA) and incubated for two hours. Sections were probed with anti-phospho-Erk1/2 (1:1000) (Sigma-Aldrich, St Louis, MO, USA) and/or anti-EGFP (1:100) (Life technologies, Carlsbad, CA, USA). Documentation of staining was performed using the Zeiss LSM510 Meta microscopy.

**Western analysis with larvae and adult liver tissue**

For the larvae total lysate, approximately 50 5 dpf larvae were lysed in RIPA buffer (31). 2.5-3.0 µl of RIPA buffer was used per larva. Total protein concentration was estimated with BCA protein assay (Piercenet, Rockford, IL, USA). Samples were denatured at 90 $^{o}$C for three minutes in laemmli buffer. 20 µg of total protein was resolved on an 8 % or 12 % SDS-polyacrylamide gel and transfer to PVDF membrane. Ras activation assay was performed with larval lysate as described in (72). For determination of mCherry-RhoA* expression in *TO(RhoA*)*, adult fish were subjected to doxycycline induction (60 µg/ml) for one week and

sacrificed. Liver tissues were harvested and lysed in T-per (Piercenet, Rockford, IL, USA) supplemented with cocktail proteinase inhibitor (Roche, Switzerland), with 25 -30 μl used per mg of tissue. The tissues were grinded with a pellet pestle for at least two minutes and incubated in the cold with strong agitation for two hours before centrifugation at maximum speed for 20 minutes at 4 °C. The supernatant was collected without the top oil layer. The total protein concentration was estimated with BCA protein assay. Samples were denatured and resolved for Western analysis.

Western analysis was performed with the following antibodies (1:1000 in TBST/BSA): anti-KRAS, anti-RhoA, anti-phospho-p21Cip and anti-p21Cip, (Santa Cruz Biotechnology, Santa Cruz, CA, USA), anti-EGFP (Invitrogen, Carlsbad, CA, USA ), anti-phospho-Erk1/2 (Sigma-Aldrich, St Louis, MO, USA), anti-Erk1/2 (BD Biosciences, San Jose, CA, USA), anti-phospho-AKT2 and anti-AKT2 (GenScript, Piscataway, NJ, USA ), anti-beta actin (Sigma-Aldrich, St Louis, MO, USA), and anti-Cox IV and anti-GAPDH (Cell Signaling Technology, Danvers, MA, USA).

**Conflict of interest.**

Authors declared no conflict of interests.

**Acknowledgments**

This work was supported by the NUS graduate research scholarship awarded to TW Chew and in part by grants from the Biomedical Research Council of Singapore (ZYG, BCL), National Medical Research Council (ZYG, BCL), and the Mechanobiology Institute of Singapore (BCL) which is co-funded through the National Research Foundation and the Ministry of Education, Singapore.

**References**


1. Cox AD, Der CJ. Ras history: The saga continues. Small Gtpases. 2010 Jul;1(1):2-27.
2. Karreth FA, Tuveson DA. Modelling oncogenic Ras/Raf signalling in the mouse. Curr Opin Genet Dev. 2009 Feb;19(1):4-11.
3. Fernandez-Medarde A, Santos E. Ras in cancer and developmental diseases. Genes Cancer. 2011 Mar;2(3):344-58.
4. Pylayeva-Gupta Y, Grabocka E, Bar-Sagi D. RAS oncogenes: weaving a tumorigenic web. Nat Rev Cancer. 2011 Oct 13.
5. Jemal A, Bray F, Center MM, Ferlay J, Ward E, Forman D. Global cancer statistics. CA Cancer J Clin. 2011 Mar-Apr;61(2):69-90.
6. Parkin DM, Bray F, Ferlay J, Pisani P. Global cancer statistics, 2002. CA Cancer J Clin. 2005 Mar-Apr;55(2):74-108.
7. Gomaa AI, Khan SA, Toledano MB, Waked I, Taylor-Robinson SD. Hepatocellular carcinoma: epidemiology, risk factors and pathogenesis. World J Gastroenterol. 2008 Jul 21;14(27):4300-8.
8. Whittaker S, Marais R, Zhu AX. The role of signaling pathways in the development and treatment of hepatocellular carcinoma. Oncogene. 2010 Sep 9;29(36):4989-5005.
9. Frau M, Biasi F, Feo F, Pascale RM. Prognostic markers and putative therapeutic targets for hepatocellular carcinoma. Mol Aspects Med. 2010 Apr;31(2):179-93.
10. Harada N, Oshima H, Katoh M, Tamai Y, Oshima M, Taketo MM. Hepatocarcinogenesis in mice with beta-catenin and Ha-ras gene mutations. Cancer Res. 2004 Jan 1;64(1):48-54.
11. Gomez del Pulgar T, Benitah SA, Valeron PF, Espina C, Lacal JC. Rho GTPase expression in tumourigenesis: evidence for a significant link. Bioessays. 2005 Jun;27(6):602-13.
12. Fukui K, Tamura S, Wada A, Kamada Y, Sawai Y, Imanaka K, et al. Expression and prognostic role of RhoA GTPases in hepatocellular carcinoma. J Cancer Res Clin Oncol. 2006 Oct;132(10):627-33.
13. Li XR, Ji F, Ouyang J, Wu W, Qian LY, Yang KY. Overexpression of RhoA is associated with poor prognosis in hepatocellular carcinoma. Eur J Surg Oncol. 2006 Dec;32(10):1130-4.

14. Wang D, Dou K, Xiang H, Song Z, Zhao Q, Chen Y, et al. Involvement of RhoA in progression of human hepatocellular carcinoma. J Gastroenterol Hepatol. 2007 Nov;22(11):1916-20.
15. Xia M, Land H. Tumor suppressor p53 restricts Ras stimulation of RhoA and cancer cell motility. Nat Struct Mol Biol. 2007 Mar;14(3):215-23.
16. Chen JC, Zhuang S, Nguyen TH, Boss GR, Pilz RB. Oncogenic Ras leads to Rho activation by activating the mitogen-activated protein kinase pathway and decreasing Rho-GTPase-activating protein activity. J Biol Chem. 2003 Jan 31;278(5):2807-18.
17. Sahai E, Olson MF, Marshall CJ. Cross-talk between Ras and Rho signalling pathways in transformation favours proliferation and increased motility. EMBO J. 2001 Feb 15;20(4):755-66.
18. Olson MF, Paterson HF, Marshall CJ. Signals from Ras and Rho GTPases interact to regulate expression of p21Waf1/Cip1. Nature. 1998 Jul 16;394(6690):295-9.
19. Zondag GC, Evers EE, ten Klooster JP, Janssen L, van der Kammen RA, Collard JG. Oncogenic Ras downregulates Rac activity, which leads to increased Rho activity and epithelial-mesenchymal transition. J Cell Biol. 2000 May 15;149(4):775-82.
20. Karaguni IM, Herter P, Debruyne P, Chtarbova S, Kasprzynski A, Herbrand U, et al. The new sulindac derivative IND 12 reverses Ras-induced cell transformation. Cancer Res. 2002 Mar 15;62(6):1718-23.
21. Qiu RG, Chen J, McCormick F, Symons M. A role for Rho in Ras transformation. Proc Natl Acad Sci U S A. 1995 Dec 5;92(25):11781-5.
22. Gupta S, Plattner R, Der CJ, Stanbridge EJ. Dissection of Ras-dependent signaling pathways controlling aggressive tumor growth of human fibrosarcoma cells: evidence for a potential novel pathway. Mol Cell Biol. 2000 Dec;20(24):9294-306.
23. Dreissigacker U, Mueller MS, Unger M, Siegert P, Genze F, Gierschik P, et al. Oncogenic K-Ras down-regulates Rac1 and RhoA activity and enhances migration and invasion of pancreatic carcinoma cells through activation of p38. Cell Signal. 2006 Aug;18(8):1156-68.
24. Pawlak G, Helfman DM. Post-transcriptional down-regulation of ROCKI/Rho-kinase through an MEK-dependent pathway leads to cytoskeleton disruption in Ras-transformed fibroblasts. Mol Biol Cell. 2002 Jan;13(1):336-47.

25. Izawa I, Amano M, Chihara K, Yamamoto T, Kaibuchi K. Possible involvement of the inactivation of the Rho-Rho-kinase pathway in oncogenic Ras-induced transformation. Oncogene. 1998 Dec 3;17(22):2863-71.
26. Amatruda JF, Shepard JL, Stern HM, Zon LI. Zebrafish as a cancer model system. Cancer Cell. 2002 Apr;1(3):229-31.
27. Beis D, Stainier DY. In vivo cell biology: following the zebrafish trend. Trends Cell Biol. 2006 Feb;16(2):105-12.
28. Feitsma H, Cuppen E. Zebrafish as a cancer model. Mol Cancer Res. 2008 May;6(5):685-94.
29. Lam SH, Gong Z. Modeling liver cancer using zebrafish: a comparative oncogenomics approach. Cell Cycle. 2006 Mar;5(6):573-7.
30. Lam SH, Wu YL, Vega VB, Miller LD, Spitsbergen J, Tong Y, et al. Conservation of gene expression signatures between zebrafish and human liver tumors and tumor progression. Nat Biotechnol. 2006 Jan;24(1):73-5.
31. Zhu S, Korzh V, Gong Z, Low BC. RhoA prevents apoptosis during zebrafish embryogenesis through activation of Mek/Erk pathway. Oncogene. 2008 Mar 6;27(11):1580-9.
32. Zhu S, Liu L, Korzh V, Gong Z, Low BC. RhoA acts downstream of Wnt5 and Wnt11 to regulate convergence and extension movements by involving effectors Rho kinase and Diaphanous: use of zebrafish as an in vivo model for GTPase signaling. Cell Signal. 2006 Mar;18(3):359-72.
33. Liu L, Zhu S, Gong Z, Low BC. K-ras/PI3K-Akt signaling is essential for zebrafish hematopoiesis and angiogenesis. PLoS One. 2008;3(8):e2850.
34. Zhu S, Low BC. Using zebrafish for studying Rho GTPases signaling in vivo. Methods Mol Biol. 2012;827:321-37.
35. Nguyen AT, Emelyanov A, Koh CH, Spitsbergen JM, Lam SH, Mathavan S, et al. A high level of liver-specific expression of oncogenic Kras(V12) drives robust liver tumorigenesis in transgenic zebrafish. Dis Model Mech. 2011 Nov;4(6):801-13.
36. Nguyen AT, Emelyanov A, Koh CH, Spitsbergen JM, Parinov S, Gong Z. An inducible krasV12 transgenic zebrafish model for liver tumorigenesis and chemical drug screening. Dis Model Mech. 2012 Jan;5(1):63-72.

37. Reboredo M, Kramer MG, Smerdou C, Prieto J, De Las Rivas J. Transcriptomic effects of Tet-on and mifepristone-inducible systems in mouse liver. Hum Gene Ther. 2008 Nov;19(11):1233-47.
38. Hancock JF. Ras proteins: different signals from different locations. Nat Rev Mol Cell Biol. 2003 May;4(5):373-84.
39. Korzh S, Pan X, Garcia-Lecea M, Winata CL, Wohland T, Korzh V, et al. Requirement of vasculogenesis and blood circulation in late stages of liver growth in zebrafish. BMC Dev Biol. 2008;8:84.
40. Mullany LK, Nelsen CJ, Hanse EA, Goggin MM, Anttila CK, Peterson M, et al. Akt-mediated liver growth promotes induction of cyclin E through a novel translational mechanism and a p21-mediated cell cycle arrest. J Biol Chem. 2007 Jul 20;282(29):21244-52.
41. Jackson LN, Larson SD, Silva SR, Rychahou PG, Chen LA, Qiu S, et al. PI3K/Akt activation is critical for early hepatic regeneration after partial hepatectomy. Am J Physiol Gastrointest Liver Physiol. 2008 Jun;294(6):G1401-10.
42. Zhou Q, Lui VW, Yeo W. Targeting the PI3K/Akt/mTOR pathway in hepatocellular carcinoma. Future Oncol. 2011 Oct;7(10):1149-67.
43. Pal I, Mandal M. PI3K and Akt as molecular targets for cancer therapy: current clinical outcomes. Acta Pharmacol Sin. 2012 Sep 17.
44. Gedaly R, Angulo P, Hundley J, Daily MF, Chen C, Evers BM. PKI-587 and sorafenib targeting PI3K/AKT/mTOR and Ras/Raf/MAPK pathways synergistically inhibit HCC cell proliferation. J Surg Res. 2012 Aug;176(2):542-8.
45. Altomare DA, Testa JR. Perturbations of the AKT signaling pathway in human cancer. Oncogene. 2005 Nov 14;24(50):7455-64.
46. Mure H, Matsuzaki K, Kitazato KT, Mizobuchi Y, Kuwayama K, Kageji T, et al. Akt2 and Akt3 play a pivotal role in malignant gliomas. Neuro Oncol. 2010 Mar;12(3):221-32.
47. O'Shaughnessy RF, Akgul B, Storey A, Pfister H, Harwood CA, Byrne C. Cutaneous human papillomaviruses down-regulate AKT1, whereas AKT2 up-regulation and activation associates with tumors. Cancer Res. 2007 Sep 1;67(17):8207-15.
48. Roy HK, Olusola BF, Clemens DL, Karolski WJ, Ratashak A, Lynch HT, et al. AKT proto-oncogene overexpression is an early event during sporadic colon carcinogenesis. Carcinogenesis. 2002 Jan;23(1):201-5.

49. Xu X, Sakon M, Nagano H, Hiraoka N, Yamamoto H, Hayashi N, et al. Akt2 expression correlates with prognosis of human hepatocellular carcinoma. Oncol Rep. 2004 Jan;11(1):25-32.
50. Rossig L, Jadidi AS, Urbich C, Badorff C, Zeiher AM, Dimmeler S. Akt-dependent phosphorylation of p21(Cip1) regulates PCNA binding and proliferation of endothelial cells. Mol Cell Biol. 2001 Aug;21(16):5644-57.
51. Li Y, Dowbenko D, Lasky LA. AKT/PKB phosphorylation of p21Cip/WAF1 enhances protein stability of p21Cip/WAF1 and promotes cell survival. J Biol Chem. 2002 Mar 29;277(13):11352-61.
52. Zhang Y, Wang Z, Magnuson NS. Pim-1 kinase-dependent phosphorylation of p21Cip1/WAF1 regulates its stability and cellular localization in H1299 cells. Mol Cancer Res. 2007 Sep;5(9):909-22.
53. Zhou BP, Liao Y, Xia W, Spohn B, Lee MH, Hung MC. Cytoplasmic localization of p21Cip1/WAF1 by Akt-induced phosphorylation in HER-2/neu-overexpressing cells. Nat Cell Biol. 2001 Mar;3(3):245-52.
54. Mebratu Y, Tesfaigzi Y. How ERK1/2 activation controls cell proliferation and cell death: Is subcellular localization the answer? Cell Cycle. 2009 Apr 15;8(8):1168-75.
55. Kim JH, Kushiro K, Graham NA, Asthagiri AR. Tunable interplay between epidermal growth factor and cell-cell contact governs the spatial dynamics of epithelial growth. Proc Natl Acad Sci U S A. 2009 Jul 7;106(27):11149-53.
56. Ming XF, Viswambharan H, Barandier C, Ruffieux J, Kaibuchi K, Rusconi S, et al. Rho GTPase/Rho kinase negatively regulates endothelial nitric oxide synthase phosphorylation through the inhibition of protein kinase B/Akt in human endothelial cells. Mol Cell Biol. 2002 Dec;22(24):8467-77.
57. Forti FL, Armelin HA. Vasopressin triggers senescence in K-ras transformed cells via RhoA-dependent downregulation of cyclin D1. Endocr Relat Cancer. 2007 Dec;14(4):1117-25.
58. Morin P, Flors C, Olson MF. Constitutively active RhoA inhibits proliferation by retarding G(1) to S phase cell cycle progression and impairing cytokinesis. Eur J Cell Biol. 2009 Sep;88(9):495-507.
59. Fleming YM, Ferguson GJ, Spender LC, Larsson J, Karlsson S, Ozanne BW, et al. TGF-beta-mediated activation of RhoA signalling is required for efficient (V12)HaRas and (V600E)BRAF transformation. Oncogene. 2009 Feb 19;28(7):983-93.

60. Khosravi-Far R, Solski PA, Clark GJ, Kinch MS, Der CJ. Activation of Rac1, RhoA, and mitogen-activated protein kinases is required for Ras transformation. Mol Cell Biol. 1995 Nov;15(11):6443-53.
61. Khosravi-Far R, White MA, Westwick JK, Solski PA, Chrzanowska-Wodnicka M, Van Aelst L, et al. Oncogenic Ras activation of Raf/mitogen-activated protein kinase-independent pathways is sufficient to cause tumorigenic transformation. Mol Cell Biol. 1996 Jul;16(7):3923-33.
62. Vidal A, Millard SS, Miller JP, Koff A. Rho activity can alter the translation of p27 mRNA and is important for RasV12-induced transformation in a manner dependent on p27 status. J Biol Chem. 2002 May 10;277(19):16433-40.
63. Skinner J, Bounacer A, Bond JA, Haughton MF, deMicco C, Wynford-Thomas D. Opposing effects of mutant ras oncoprotein on human fibroblast and epithelial cell proliferation: implications for models of human tumorigenesis. Oncogene. 2004 Aug 5;23(35):5994-9.
64. Man JH, Liang B, Gu YX, Zhou T, Li AL, Li T, et al. Gankyrin plays an essential role in Ras-induced tumorigenesis through regulation of the RhoA/ROCK pathway in mammalian cells. J Clin Invest. 2010 Aug 2;120(8):2829-41.
65. Shah V, Bharadwaj S, Kaibuchi K, Prasad GL. Cytoskeletal organization in tropomyosin-mediated reversion of ras-transformation: Evidence for Rho kinase pathway. Oncogene. 2001 Apr 19;20(17):2112-21.
66. Her GM, Chiang CC, Chen WY, Wu JL. In vivo studies of liver-type fatty acid binding protein (L-FABP) gene expression in liver of transgenic zebrafish (Danio rerio). FEBS Lett. 2003 Mar 13;538(1-3):125-33.
67. Li Z, Huang X, Zhan H, Zeng Z, Li C, Spitsbergen JM, et al. Inducible and repressable oncogene-addicted hepatocellular carcinoma in Tet-on xmrk transgenic zebrafish. J Hepatol. 2011 Aug 31.
68. Emelyanov A, Gao Y, Naqvi NI, Parinov S. Trans-kingdom transposition of the maize dissociation element. Genetics. 2006 Nov;174(3):1095-104.
69. Westerfield M. The zebrafish book. A guide for the laboratory use of zebrafish (Danio rerio). 4th ed.: Univ. of Oregon Press, Eugene.; 2000.
70. Spitsbergen JM, Peterson TS, Buhler. DR. Neoplasia in laboratory zebrafish. ILAR Journal. 2012:In press.

71. Boorman GA, Botts S, Bunton TE, Fournie JW, Harshbarger JC, Hawkins WE, et al. Diagnostic criteria for degenerative, inflammatory, proliferative nonneoplastic and neoplastic liver lesions in medaka (Oryzias latipes): consensus of a National Toxicology Program Pathology Working Group. Toxicol Pathol. 1997 Mar-Apr;25(2):202-10.
72. Ravichandran A, Low BC. SmgGDS antagonizes BPGAP1-induced Ras/ERK activation and neuritogenesis in PC12 cells differentiation. Mol Biol Cell. 2012 Nov 14.

**Figure 1: Characterization of the *TO(Kras$^{G12V}$)*** (A) Image demonstrated liver-specific expression of EGFP-Kras$^{G12V}$ in the transgenic 6 dpf larvae after doxycycline exposure. (B) Western blots of whole embryo lysate of EGFP-positive and EGFP-negative 5 dpf larvae. Both panels showed a band corresponding to approximately 50 KDa in the EGFP-positive larval lysate when probed with anti-KRAS antibody and anti-EGFP antibody. No corresponding band was observed in the EGFP-negative larvae lysate (wild-type sibling control). (C) Active RAS-RBD pull-down assay followed by Western indicated that the ectopically expressed EGFP-Kras$^{G12V}$ protein (~50 KDa) was GTP-bound and active. Blots were first probed with anti-EGFP antibody and developed; stripped and re-probed with anti-KRAS antibody for the second development of blots. (D) Cross-section of EGFP-positive transgenic 6 dpf larva imaged by confocal microscopy. The ectopically expressed EGFP-Kras$^{G12V}$ proteins were predominantly distributed to the plasma membrane. Section was counterstained with DAPI to illustrate the nucleus.

**Figure 2: Oncogenic Kras expression in the liver caused an enlargement of the organ through increased hepatocyte proliferation**. (A) Volumetric analyses of the liver in the Lipan liver vs *TO(Kras$^{G12V}$)*. Liver-specific expression of EGFP-Kras$^{G12V}$ caused significant increase in the organ size (volume) as compared to the control. (** denotes: p-value < 0.01; n = 12). Error bars represent standard deviation. (B) Proliferative index was scored based on number of pH3 stained cells over the area occupied by the liver. The bar chart plotted relative ratio vs genotypes. The wild-type was set as the reference value of one. Oncogenic Kras increased the hepatocyte proliferation significantly as compared to the wild-type. (n = 4; ** denotes: p-value < 0.01).

Insert: Significantly more pH3 positive cells were observed in the *TO(Kras$^{G12V}$)* compared to the wild-type. The livers of wild-type and TO(KrasG12V) were highlighted with yellow dots. pH3 positive cells were stained pink. Error bar denotes standard deviation.

**Figure 3: EGFP-Kras$^{G12V}$ expression increased activation of the RAF/MEK/Erk and PI3K/Akt2 signaling.** Larvae from out-cross of *TO(Kras$^{G12V}$)* with wild-type were analyzed. Approximately 50 larvae were pooled for each genotype (lane) per Western analysis. Immunoblots representative of at least three repeats. They were probed for phospho-Erk1/2, total Erk 1/2, phospho-Akt2, total Akt2, phospho-p21Cip and total-p21Cip. (A) There was an increased in the amount of phospo-Erk1/2 in the EGFP-Kras$^{G12V}$ expressing larvae, while the total Erk 1/2 level remained relatively similar. (B) There were an increase in both the amount of phospho-Akt2 and total Akt2 in the EGFP-Kras$^{G12V}$ larvae compared to their wild-type siblings. (C) There was an increase in the level of phosphorylation of p21Cip in the EGFP-Kras$^{G12V}$ expressing larvae compared to their wild-type siblings. β-actin was used to demonstrate equal loading.

**Figure 4: Formation of hepatocellular carcinomas (HCC) in adult fish upon the induction of the EGFP-Kras$^{G12V}$ transgene in the *TO(Kras$^{G12V}$)* line.** The genotypes of the fish and the treatment dosages of doxycycline were labelled at the top. (A-C) Fish were dissected to illustrate the size of the liver. The livers were highlighted with the dotted yellow line. There was obvious enlargement of the liver in Figure 4A compared to Figures 4B & C. (D-F) H&E staining of the

Bouin's fixed paraffin sections. Figure 4D illustrated features that are characteristic of HCC, while the Figure 4E & F showed no significant lesions. (G-I) Immunohistochemical (IHC) staining of the paraffin section with proliferation marker, PCNA (brown). Figure 4G showed a significant increase in the staining as compared to Figures 4H & I. (J & K) Increased phospho-Erk1/2 staining was observed in the *TO(Kras$^{G12V}$)* compared to the wild-type control. The staining of the phosho-Erk1/2 was mainly observed in the nucleus. Scale bar for Figure 4A to F is one cm. Scale bar for Figure 4D to K is 50 μm.

**Figure 5: Characterization of *TO(RhoA*)* lines.** (A-C) Liver specific expression of mCherry-RhoA (or its mutants) was demonstrated upon induction by doxycycline. Respective genotypes of the larvae were labelled on the top. (D-F) Western analyses of the liver lysate from adult transgenic fish and their wild-type siblings after doxycycline induction. When probed with anti-RhoA antibody, all three transgenic lines showed a band of approximately 50 KDa (mCherry and RhoA fusion protein), which was not present in the wild-type siblings. (G-I) Confocal images of the respective transgenic lines demonstrated live-specific expression of the mCherry-tagged proteins in the three transgenic RhoA lines.

**Figure 6: Effects of RhoA or its mutant on Kras$^{G12V}$ induced liver overgrowth.** (A-C) Volumetric analyses on the effect of RhoA signaling on Kras$^{G12V}$-mediated liver enlargement. The larvae were analyzed from the same family to account for the genetic background effects and variation in environment on growth. (A) RhoA$^{T19N}$ augmented the Kras$^{G12V}$-mediated liver enlargement significantly, while (B) the RhoA$^{G14V}$ reduced it significantly. (C) No significant change in liver volume was observed in the double transgenic *TO(Kras$^{G12V}$/RhoA)* compared to the *TO(Kras$^{G12V}$)* larvae. n ≥ 50 in Figure 6B and C. n ≥ 80 in Figure 6A (** denotes p-value < 0.01). Error bars denote standard deviation. (D-F) Larvae were induced with doxycycline at 2 dpf and harvested at 5 dpf for western analysis probing for phospho-Akt2 and Akt2. Approximately 50 larvae were pooled for each genotype (lane) per Western analysis. Immunoblots were representative of at least three repeats. (D) The co-expression of RhoA$^{T19N}$ with Kras$^{G12V}$ caused a slight increase in both the Akt2 expression and activities. The upper panel displayed a higher exposure compared to the second panel probed with anti-phospho-Akt2 while (E) co-expression of RhoA$^{G14V}$ caused a significant reduction in oncogenic Kras-induced Akt2 expression and activities. (F) Co-expression of RhoA did not affect the Kras$^{G12V}$-induced Akt2 upregulation and activities. Cox IV was used as loading control.

**Figure 7: Effects of RhoA signaling on oncogenic Kras-mediated HCC development.** (A) Survival analyses of the different genotypes. The Kaplan-meier plot showed days post induction plotted against percentage survival. The dosage of doxycycline used was 10 μg/ml and the treatment was stopped at 75 days. No death was observed in the wild-type and three single transgenic of *TO(RhoA), TO(RhoA$^{G14V}$),* and *TO(RhoA$^{T19N}$)* at the end of the treatment. The expression of Kras$^{G12V}$ (black line) in the liver caused a significant decline in survival compared to the wild-type and the three single transgenic RhoA transgenic fish (grey line). The double transgenic of *TO(Kras$^{G12V}$/RhoA$^{T19N}$)* (blue line) accelerated death significantly compared to the single *TO(Kras$^{G12V}$)* (black line); double transgenic *TO(Kras$^{G12V}$/RhoA)* (red line) and *TO(Kras$^{G12V}$/RhoA$^{G14V}$)* (yellow line). No significant changes were observed in the *TO(Kras$^{G12V}$)* vs the double transgenic of *TO(Kras$^{G12V}$/RhoA)* and *TO(Kras$^{G12V}$/RhoA$^{G14V}$)*, respectively. No death event was recorded for the non-doxycycline control groups. Different letters in red represent p-value < 0.01. (B-Q) Formations of liver tumors were observed in transgenic zebrafish which expressed EGFP-Kras$^{G12V}$. The genotype and dosage of doxycycline are labeled on top of the images. The fish with the most severe phenotypes were represented in this figure. (B-E) Fish were dissected to visualize the liver. The livers are highlighted with the yellow dotted line. All the fish have enlarged livers. (F-I) H&E staining of the Bouin's-fixed paraffin sections displayed characteristic features of HCC. (J-M) IHC staining was performed with anti-PCNA to demonstrate the accompanied increased hepatocyte proliferation in the HCC samples. Slides were counterstained with hematoxylin. The *TO(Kras$^{G12V}$/RhoA$^{T19N}$)* transgenic fish demonstrated an apparently higher proliferation rate than the other three transgenic lines. Scale bar: A to I is one cm, J to M is 50 μm and N to Q is 100 μm.

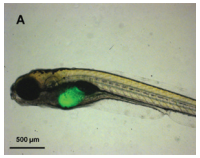
A
500 µm

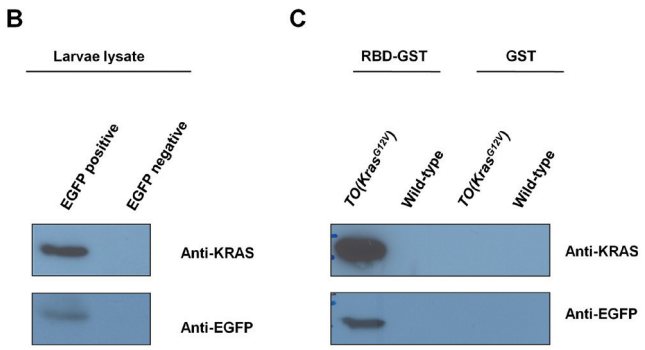
B
Larvae lysate
EGFP positive
EGFP negative
Anti-KRAS
Anti-EGFP
C
RBD-GST
GST
TO(KrasG12V)
Wild-type
TO(KrasG12V)
Wild-type
Anti-KRAS
Anti-EGFP

**D**

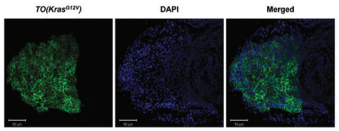

A

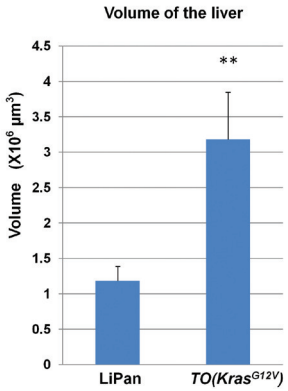
Volume of the liver
Volume (X10^6 µm^3)
4.5
4
3.5
3
2.5
2
1.5
1
0.5
0
**
LiPan
TO(KrasG12V)

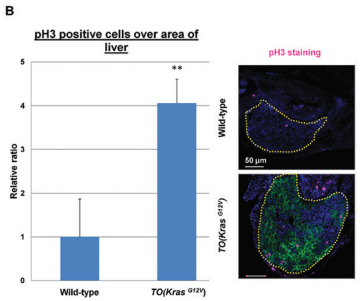
B
pH3 positive cells over area of liver
Relative ratio
5
4
3
2
1
0
**
Wild-type
TO(Kras G12V)
pH3 staining
Wild-type
TO(Kras G12V)
50 μm

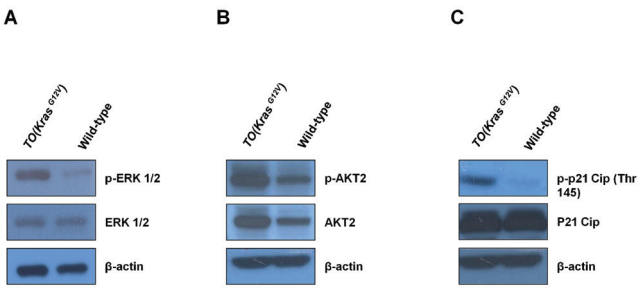
A
TO(Kras G12V)
Wild-type
p-ERK 1/2
ERK 1/2
β-actin
B
TO(Kras G12V)
Wild-type
p-AKT2
AKT2
β-actin
C
TO(Kras G12V)
Wild-type
p-p21 Cip (Thr 145)
P21 Cip
β-actin

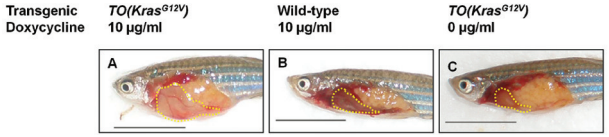
Transgenic
Doxycycline
TO(KrasG12V)
10 µg/ml
Wild-type
10 µg/ml
TO(KrasG12V)
0 µg/ml
A
B
C

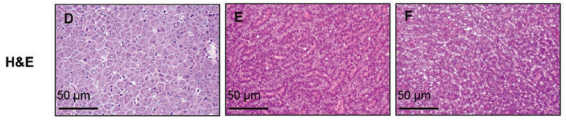
H&E
D
50 µm
E
50 µm
F
50 µm

PCNA

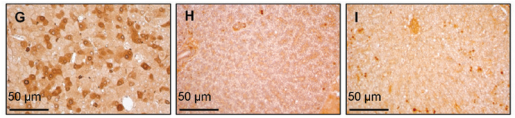

p-Erk1/2

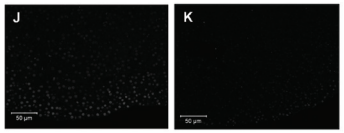

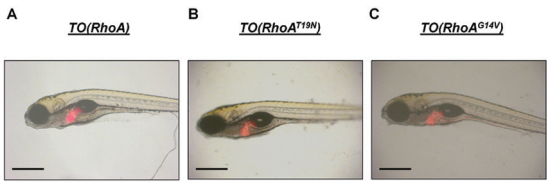
A
TO(RhoA)
B
TO(RhoA$^{T19N}$)
C
TO(RhoA$^{G14V}$)

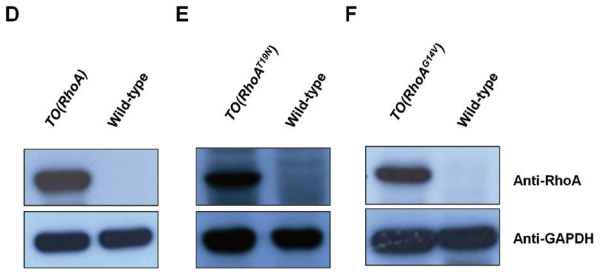
D
E
F
TO(RhoA)
Wild-type
TO(RhoA^T19N)
Wild-type
TO(RhoA^G14V)
Wild-type
Anti-RhoA
Anti-GAPDH

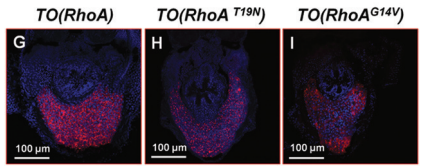
TO(RhoA)
TO(RhoA T19N)
TO(RhoAG14V)
G
H
I
100 µm
100 µm
100 µm

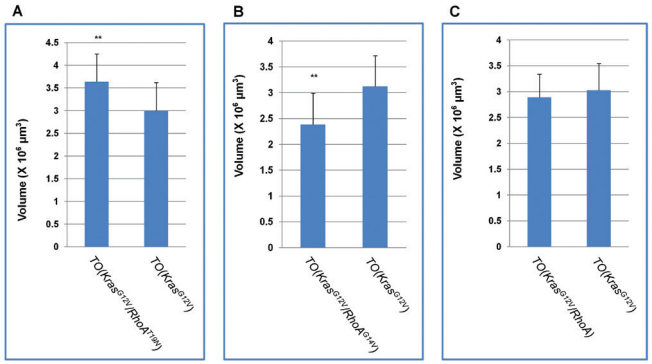
A
B
C
Volume (X 10⁶ µm³)
**
TO(KrasG12V/RhoAY99A)
TO(KrasG12V)
TO(KrasG12V/RhoAG14V)
TO(KrasG12V/RhoA)

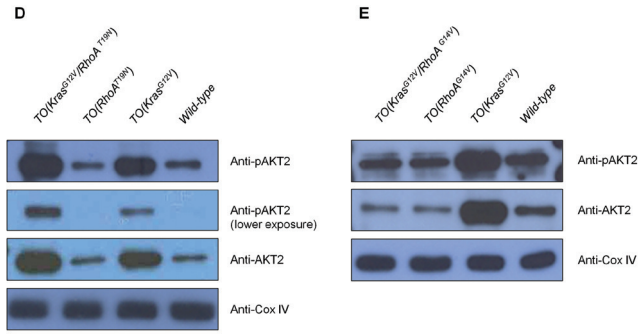
D
TO(KrasG12V/RhoA T19N)
TO(RhoAT19N)
TO(KrasG12V)
Wild-type
Anti-pAKT2
Anti-pAKT2
(lower exposure)
Anti-AKT2
Anti-Cox IV
E
TO(KrasG12V/RhoA E40Y)
TO(RhoAE40Y)
TO(KrasG12V)
Wild-type
Anti-pAKT2
Anti-AKT2
Anti-Cox IV

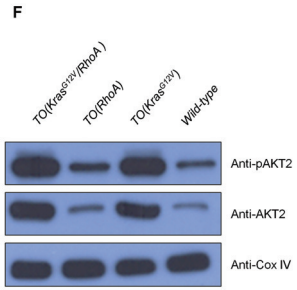
F
TO(Kras$^{G12V}$/RhoA)
TO(RhoA)
TO(Kras$^{G12V}$)
Wild-type
Anti-pAKT2
Anti-AKT2
Anti-Cox IV

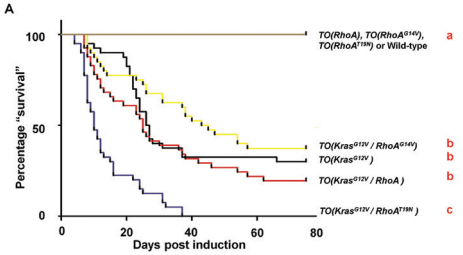
A
100
50
0
Percentage "survival"
0
20
40
60
80
Days post induction
TO(RhoA), TO(RhoA^G14V), TO(RhoA^T19N) or Wild-type
a
TO(Kras^G12V / RhoA^G14V)
b
TO(Kras^G12V )
b
TO(Kras^G12V / RhoA )
b
TO(Kras^G12V / RhoA^T19N )
c

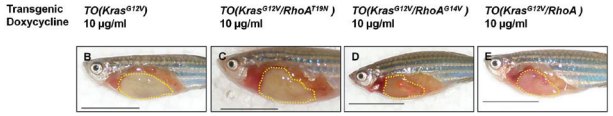
Transgenic
Doxycycline
TO(KrasG12V)
10 µg/ml
TO(KrasG12V/RhoAT19N )
10 µg/ml
TO(KrasG12V/RhoAG14V )
10 µg/ml
TO(KrasG12V/RhoA )
10 µg/ml
B
C
D
E

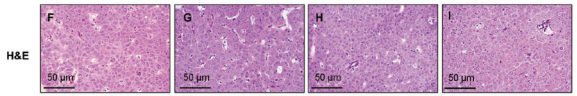
H&E
F
G
H
I
50 µm
50 µm
50 µm
50 µm

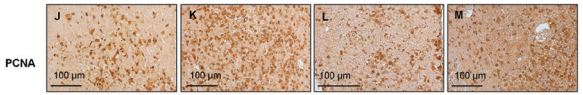
PCNA
J
K
L
M
100 µm
100 µm
100 µm
100 µm